Inorg. Chem. **2009**, *48*, 1423−1432

Crystal Structures of Titanate Nanotubes: A Raman Scattering Study

Tao Gao,* Helmer Fjellvåg, and Poul Norby

Centre for Materials Science and Nanotechnology and Department of Chemistry, University of Oslo, P.O. Box 1033, N-0315 Oslo, Norway

Received August 8, 2008

Crystal structures of titanate nanotubes prepared from a NaOH treatment of TiO_2 with subsequent acid washing were discussed from a viewpoint of vibrational spectroscopy. The correlation between the vibrational feature and the polymerization nature of the TiO_6 octahedron was established by analyzing Raman scattering data of crystalline TiO_2 (anatase and rutile) and layered protonic titanates. Then, the polymerization nature of TiO_6 octahedra in the titanate nanotubes was identified by comparing their Raman scattering spectra with those of the crystalline TiO_2 and layered protonic titanates. It demonstrated that the titanate nanotubes consist of two-dimensional TiO_6 octahedral host layers with a lepidocrocite (γ-FeOOH)-type layered structure. This conclusion was confirmed further by considering the Raman scattering properties of a restacked titanate prepared by assembling TiO_6 octahedral layers derived from the original scroll-like titanate nanotubes. Our findings offered a convenient approach to validate the crystal structures of the products from an alkaline treatment of TiO_2 under different experimental conditions.

Introduction

Since the first report of TiO_2-based nanotubes prepared via a simple wet chemical method, that is, a NaOH treatment of crystalline TiO_2 powders with subsequent washing,[1] significant interest has been given to this novel nanostructure due to its wide range of practical applications as photocatalysts,[2] sensors,[3,4] electrochemical capacitors,[5] and lithium-inserting materials.[6,7] Another point of interest is the crystal structure of the TiO_2-based nanotubes, which is still under debate. So far, several distinct structural models based on tetragonal anatase TiO_2,[1,8,9] monoclinic $H_2Ti_3O_7$,[5,10−14] monoclinic $H_2Ti_4O_9$,[15] orthorhombic $H_2Ti_2O_5\cdot H_2O$,[16,17] and orthorhombic $H_{0.7}Ti_{1.825}\square_{0.175}O_4\cdot H_2O$ ($\square$: vacancy)[18] have been proposed to represent the crystal structure of the nanotubes. The controversy still goes on. Obviously, further efforts devoted to understanding the microstructure of the TiO_2-based nanotubes are still necessary.

Originally, Kasuga et al. thought that the phase structure of the TiO_2-based nanotubes was crystalline TiO_2.[1] This conclusion was followed by subsequent studies.[8,9] For example, Yao et al. suggested that, during the alkaline treatment, three-dimensional (3D) anatase TiO_2 crystallites

* To whom correspondence should be addressed. E-mail: tao.gao@kjemi.uio.no.

(1) Kasuga, T.; Hiramatsu, M.; Hoson, A.; Sekino, T.; Niihara, K. *Adv. Mater.* **1999**, *11*, 1307. Kasuga, T.; Hiramatsu, M.; Hoson, A.; Sekino, T.; Niihara, K. *Langnuir* **1998**, *14*, 3160.
(2) Adachi, M.; Murata, Y.; Harada, M.; Yoshikawa, S. *Chem. Lett.* **2000**, 942.
(3) Liu, S.; Chen, A. *Langmuir* **2005**, *21*, 8409.
(4) Varghese, O. K.; Gong, D.; Paulose, M.; Ong, K. G.; Dickey, E. C.; Grimes, C. A. *Adv. Mater.* **2003**, *15*, 624.
(5) Wang, Y. G.; Zhang, X. G. *J. Electrochem. Soc.* **2005**, *152*, A671. Wang, Y. G.; Zhang, X. G. *Electrochim. Acta* **2004**, *49*, 1957.
(6) Armstrong, G.; Armstrong, A. R.; Canales, J.; Bruce, P. G. *Chem. Commun.* **2005**, 2454.
(7) Zhang, H.; Li, G. R.; An, L. P.; Yan, T. Y.; Gao, X. P.; Zhu, H. Y. *J. Phys. Chem. C* **2007**, *111*, 6143.
(8) Yao, B. D.; Chan, Y. F.; Zhang, X. Y.; Zhang, W. F.; Yang, Z. Y.; Wang, N. *Appl. Phys. Lett.* **2003**, *82*, 281.
(9) Wang, Y. Q.; Hu, G. Q.; Duan, X. F.; Sun, H. L.; Xue, Q. K. *Chem. Phys. Lett.* **2002**, *365*, 427.
(10) Du, G. H.; Chen, Q.; Che, R. C.; Yuan, Z. Y.; Peng, L.-M. *Appl. Phys. Lett.* **2001**, *79*, 3702. Chen, Q.; Zhou, W.; Du, G.; Peng, L. M. *Adv. Mater.* **2002**, *14*, 1208. Chen, Q.; Du, G. H.; Zhang, S.; Peng, L. M. *Acta Crystallogr.* **2002**, *B58*, 587.
(11) Zhang, S.; Peng, L.-M.; Chen, Q.; Du, G. H.; Dawson, G.; Zhou, W. Z. *Phys. Rev. Lett.* **2003**, *91*, 256103. Zhang, S.; Chen, Q.; Peng, L.-M. *Phys. Rev. B: Condens. Matter Mater. Phys.* **2005**, *71*, 014104.
(12) Sun, X.; Li, Y. *Chem.—Eur. J.* **2003**, *9*, 2229.
(13) Thorne, A.; Kruth, A.; Tunstall, D.; Irvine, J. T. S.; Zhou, W. *J. Phys. Chem. B* **2005**, *109*, 5439.
(14) Wu, D.; Liu, J.; Zhao, X.; Li, A.; Chen, Y.; Ming, N. *Chem. Mater.* **2006**, *18*, 547.
(15) Nakahira, A.; Kato, W.; Tamai, M.; Isshiki, T.; Nishio, K. *J. Mater. Sci.* **2004**, *39*, 4239.
(16) Yang, J.; Jin, Z.; Wang, X.; Li, W.; Zhang, J.; Zhang, S.; Guo, X.; Zhang, Z. *Dalton Trans.* **2003**, 3898.
(17) Tsai, C. C.; Teng, H. *Chem. Mater.* **2006**, *18*, 367. Nian, J. N.; Teng, H. *J. Phys. Chem. B* **2006**, *110*, 4193.
(18) Ma, R.; Bando, Y.; Sasaki, T. *Chem. Phys. Lett.* **2003**, *380*, 577. Ma, R.; Sasaki, T.; Bando, Y. *Chem. Commun.* **2005**, 948. Ma, R.; Fukuda, K.; Sasaki, T.; Osada, M.; Bando, Y. *J. Phys. Chem. B* **2005**, *109*, 6210.

10.1021/ic801508k CCC: $40.75
Published on Web 01/14/2009

were delaminated into two-dimensional (2D) lamellar TiO_2 sheets, and those were subsequently transformed or rolled into one-dimensional (1D) scroll-like anatase TiO_2 nanotubes.[8] This 3D to 1D transformation was also reported by Wang et al. according to detailed high-resolution transmission electron microscopy (HR-TEM) analyses.[9] However, this TiO_2-type model is not satisfactory since crystalline TiO_2, either anatase or rutile, does not possess any layers that can form the walls of the final tubes.[10−18] It has recently been realized that the nanotubes obtained by the NaOH treatment of TiO_2 with subsequent washing and ion-exchange are actually layered protonic titanates,[10−18] of which, however, details are still in debate. For example, Peng et al. proposed that the crystal structure of the titanate nanotubes could be described as a monoclinic trititanate $H_2Ti_3O_7$,[10,11] which has widely been followed by other researchers.[12−14] An atomic pair distribution function (PDF) analysis, which is known to be well-suited for materials with limited structural coherence,[19] was also conducted to understand the microstructure of the titanate nanotubes,[20] and it was found that the $H_2Ti_3O_7$-type model yields better results during the PDF simulations. On the other hand, a different monoclinic titanate, tetratitanate $H_2Ti_4O_9 \cdot H_2O$, was reported by Nakahira and coauthors to represent the crystal structure of the titanate nanotubes.[15] Note that these monoclinic titanates, $H_2Ti_nO_{2n+1}$ ($n = 3, 4$), are structurally similar: both of them are composed of parallel corrugated ribbons of edge-sharing TiO_6 octahedra stepped by n octahedra. In contrast to these monoclinic titanates, structural models based on orthorhombic titanates were also reported.[16−18] For example, Yang et al. propounded that the titanate nanotubes prepared from the NaOH treatment of TiO_2 were $Na_{2-x}H_xTi_2O_4(OH)_2$, where x depends on the pH of the post-treatment solution.[16] Similar results were reported later by Tsai and Teng;[17] they concluded that a divalent protonic titanate, $H_2Ti_2O_5 \cdot H_2O$, was the structural basis of the protonic titanate nanotubes.[17] Ma et al. proposed a different orthorhombic titanate, $H_{0.7}Ti_{1.825}\square_{0.175}O_4 \cdot H_2O$, as the crystal structure of the titanate nanotubes.[18] It is worth pointing out that both $H_2Ti_2O_5 \cdot H_2O$ (or $H_2Ti_2O_4(OH)_2$) and $H_{0.7}Ti_{1.825}\square_{0.175}O_4 \cdot H_2O$ consist of similar lepidocrocite (γ-FeOOH)-type TiO_6 octahedral host layers but with different proton contents. On the basis of molecular dynamics calculations, Alvarez-Ramirez and Ruiz-Morales demonstrated that the transformation of lepidocrocite-type titanates from the hydrothermal treatment of TiO_2 with NaOH is energetically favorable.[21] Moreover, the formation of titanate nanotubes from a low-temperature acid treatment of orthorhombic lepidocrocite-type sodium titanates, $Na_{0.54}Ti_{1.865}\square_{0.135}O_4$, was reported recently.[22]

We wish to make it clear that, so far, the proposed structural models for the titanate nanotubes are mainly based on X-ray and electron crystallography, including X-ray diffraction (XRD), electron diffraction (ED), HR-TEM, and so forth. However, due to the poor crystallinity of the nanotubes, a complete and reliable description on their crystal structures via these conventional diffraction methods remains difficult. For example, the characteristic XRD reflections (or ED spots/rings) of the titanate nanotubes are frequently few in number, broad, and sometimes variable in position and do not serve as a satisfactory basis for structure identification. On the other hand, the protonic titanate nanotubes tend to dehydration under high-energy electron beam irradiation, which will result in a certain degree of shrinkage in the interplanar distance; consequently, lattice parameters estimated from the ED or HR-TEM data might not be accurate enough for a reliable structural model. Other characterization techniques that can contribute to an understanding of crystal structures of materials will be of great interest as well as importance in the structural studies of the titanate nanotubes. We suggest, in this regard, that the crystal structure of the titanate nanotubes could be understood with the help of vibrational spectroscopic methods such as Raman scattering, which is a necessary alternative and a useful supplement to the diffraction approaches such as XRD for accessing a deeper structural description of a given material. Actually, Ma et al. revealed previously the difference between monoclinic trititanate $H_2Ti_3O_7$ and orthorhombic lepidocrocite titanate $H_{0.7}Ti_{1.825}\square_{0.175}O_4 \cdot H_2O$ via Raman scattering and X-ray absorption fine structure;[18] however, detailed analyses on the Raman scattering data of these titanates and the titanate nanotubes were still not available.

So far, Raman scattering data of the titanate nanotubes have been widely reported;[1,8,12,18,22−25] however, their contributions to the understanding of the crystal structures are very limited. Kasuga et al. attributed previously the well-defined Raman bands of the nanotubes to Ti−O vibrations that appear in crystalline TiO_2 (anatase or rutile) with similar band positions.[1] This methodology was followed in subsequent studies.[23−25] In such a way, however, it is impossible to correlate the vibrational feature of the titanate nanotubes to their structural properties such as the polymerization nature of the TiO_6 octahedron in the nanotubular framework. An analysis of the vibration species in terms of symmetry properties is required but unfortunately not achieved so far for the titanate nanotubes. The difficulty is obvious: it is still not clear how the Raman scattering properties of flat titanate nanosheets change as they transform into scroll-like nanotubes. The rolling process is believed to result in some local structural evolutions, such as changes of the corresponding Ti−O bond lengths and bond angles; lattice vibrations related to these Ti−O bonds will be modified subsequently. These local structural evolutions must be evaluated to achieve an improved understanding of the crystal structure of the titanate

(19) Gateshki, M.; Hwang, S. J.; Park, D. H.; Ren, Y.; Petkov, V. *Chem. Mater.* **2004**, *16*, 5153. Gateshki, M.; Yin, S.; Ren, Y.; Petkov, V. *Chem. Mater.* **2007**, *19*, 2512.
(20) Gateshki, M.; Chen, Q.; Peng, L. M.; Chupas, P.; Petkov, V. *Z. Kristallogr.* **2007**, *222*, 612. Pradhan, S. K.; Mao, Y.; Wong, S. S.; Chupas, P.; Petkov, V. *Chem. Mater.* **2007**, *19*, 6180.
(21) Alvarez-Ramirez, F.; Ruiz-Morales, Y. *Chem. Mater.* **2007**, *19*, 2947.
(22) Tsai, C. C.; Teng, H. *Langmuir* **2008**, *24*, 3434.
(23) Hodos, M.; Horváth, E.; Haspel, H.; Kukovecz, Á.; Kónya, Z.; Kiricsi, I. *Chem. Phys. Lett.* **2004**, *399*, 512.
(24) Qian, L.; Du, Z. L.; Yang, S. Y.; Jin, Z. S. *J. Mol. Struct.* **2005**, *749*, 103.
(25) Menzel, R.; Peiró, A. M.; Durrant, J. R.; Shaffer, M. S. P. *Chem. Mater.* **2006**, *18*, 6059.

nanotubes; however, it is difficult since the rolling process is performed under somewhat unconventional conditions[11] and can hardly be monitored by vibrational spectroscopy.

We are interested in examining the reliability of the structural models proposed for the titanate nanotubes via vibrational spectroscopy; Raman scattering is mainly employed since it is more convenient than IR spectroscopy.[26,27] By analyzing Raman scattering properties of the crystalline TiO_2 (anatase and rutile) and several layered protonic titanates, we establish first the correlation between the vibrational feature and the polymerization nature of TiO_6 octahedra in these compounds. Then, we assemble a restacked titanate by employing the individual TiO_6 octahedral host layers derived from the original scroll-like titanate nanotubes.[27] By comparing the Raman scattering data of the titanate nanotubes, the crystalline TiO_2, the layered protonic titanates, and the restacked titanates, we are able to identify the polymerization nature of TiO_6 octahedra in the titanate nanotubes. We demonstrate that the crystal structure of the titanate nanotubes can be better described as the protonic titanate $H_{0.7}Ti_{1.825}\square_{0.175}O_4 \cdot H_2O$ with a lepidocrocite-type layered structure.[18,22] Because different titanate structures might be obtained via the NaOH treatment of TiO_2 under different experimental conditions,[14,18,28,29] the application of vibrational methods such as Raman scattering seems necessary and important to collect sufficient evidence for a reliable description on the crystal structures of the final products.

Experimental Section

Reagents and Materials. Cesium carbonate, Cs_2CO_3 (99.9%); sodium carbonate, Na_2CO_3 (99%); potassium carbonate, K_2CO_3 (99%); anatase-type TiO_2 (99.7%); and tetramethylammonium ($(C_4H_9)_4N^+$, abbreviated as TMA hereafter) hydroxide aqueous solution (25 wt %) were purchased from Sigma-Aldrich Co. and used as received.

Synthesis. Titanate Nanotubes. The titanate nanotubes used in this work were synthesized by following the procedure developed by Kasuga et al.[1] with a small modification. For a typical synthesis, TiO_2 powders (0.5 g) were added to an aqueous solution of NaOH (10 M, 100 mL). After being stirred at room temperature for 30 min, the produced white suspension was charged into Teflon-lined autoclaves and heated to 140 °C for 24−72 h without shaking or stirring. After the autoclave had been cooled down to room temperature with tap water, the white precipitates were filtered and then acid-washed, which involved stirring the products in a 0.2 M HNO_3 aqueous solution for three days. The acid solution was renewed daily to promote a complete ion exchange. After the acid washing, the material was filtered, washed with water, and dried at 80 °C overnight to give the as-prepared titanate nanotubes.

Unscrolling-Restacking. The as-prepared titanate nanotubes were first unscrolled into corresponding titanate nanosheets by ion intercalation with organic amine ions, the details of which were reported previously.[27] In this study, the as-prepared titanate nanotubes (50 mg) were ultrasonically dispersed in 50 mL of a TMAOH aqueous solution (10 wt %), which has been found to be very efficient for the unscrolling of nanotubes (see the Supporting Information). After being ultrasonically treated for 1 h, the obtained suspension was stirred at 50 °C for 7 days to produce a stable colloidal titanate nanosheet suspension. For the preparation of restacked titanates, 20 mL of the colloidal titanate nanosheet suspension was poured into 200 mL of a HNO_3 aqueous solution (1M) under vivid stirring. Some alkaline solutions (1 M NaOH and 1 M KOH) were also employed (see the Supporting Information). A wool-like precipitate was formed immediately upon mixing. The solid products were then filtered and washed through with water. Freeze-drying of the solid products yielded a voluminous cottonlike solid. The products are denoted as restacked titanates hereafter.

Anatase and Rutile. The crystalline TiO_2 powders were obtained by heating the as-prepared titanate nanotubes in the air at 600 °C (for anatase) or 800 °C (for rutile) for 2 h.

Layered Titanates. The bulky layered titanates $A_2Ti_nO_{2n+1}$ ($n = 3$, A = Na; $n = 4$, A = K; $n = 6$, A = Cs) were prepared using conventional solid-state calcination. Stoichiometric quantities of alkali metal carbonate (Na_2CO_3, K_2CO_3, and Cs_2CO_3) and TiO_2 were ground under acetone with a mortar and pestle. Thereafter, the well-mixed powders were pelleted and heated in the air at 800 °C for 40 h. The as-prepared titanates were white microcrystallites with fiber- or platelike morphologies. Protonic forms of the obtained alkali metal titanates were prepared by ion exchange, which involved stirring the titanate powders (200 mg) in a 1 M H_2SO_4 aqueous solution (200 mL) for three days. The acid solution was renewed daily to promote a complete ion exchange. Finally, the solid materials were filtered, washed with water, and dried at room temperature to give the as-prepared protonic titanates, $H_2Ti_nO_{2n+1} \cdot yH_2O$. Note that the $Cs_2Ti_6O_{13}$ is actually $Cs_{0.7}Ti_{1.825}\square_{0.175}O_4$ with a lepidocrocite-type layered structure;[30] the acid-exchange results in the corresponding protonic titanate gave $H_{0.7}Ti_{1.825}\square_{0.175}O_4 \cdot H_2O$. Moreover, the preparation of divalent protonic titanate $H_2Ti_2O_5 \cdot H_2O$ following the procedures reported in ref 31 was tried several times but failed in the present study.

Characterization. Phase analysis and crystal structure data of the obtained materials were based on powder XRD collected on a Siemens D5000 powder diffractometer (Cu $K\alpha_1$ radiation $\lambda = 0.15405$ nm; PSD detector; reflection geometry). The morphology and composition of the samples were analyzed by scanning electron microscopy (SEM, FEI Quanta 200F) and transmission electron microscopy (Philips CM30ST) equipped with an energy-dispersive X-ray spectrometer. The surface area and mesoporous structure of titanate nanotubes were characterized by nitrogen isothermal adsorption at 77 K using a BELSORP high-precision adsorption measuring apparatus. The surface area of the nanotubes was determined from the Brunauer−Emmett−Teller (BET) equation and the pore volume from the total amount adsorbed at relative pressures near unity. The pore size distribution was analyzed by using the Barrett−Joyner−Halenda (BJH) method. Thermogravimetric analysis (TGA) of the as-prepared titanate nanotubes was carried out on a Perkin-Elmer TGA 7 system at a heating rate of 5 °C/min under a N_2 flow. Fourier transform infrared (FT-IR) spectra were recorded for samples prepared via the standard KBr technique on a PerkinElmer Spectrum 2000 FT-IR spectrometer (resolution: 2

(26) Gao, T.; Fjellvåg, H.; Norby, P. *J. Phys. Chem. B* **2008**, *112*, 9400.
(27) Gao, T.; Wu, Q. L.; Fjellvåg, H.; Norby, P. *J. Phys. Chem. C* **2008**, *112*, 8548.
(28) Papp, S.; Kõrösi, L.; Meynen, V.; Cool, P.; Vansant, E. F.; Dékány, I. *J. Solid State Chem.* **2005**, *178*, 1614. Kolen'ko, Y. V.; Kovnir, K. A.; Gavrilov, A. I.; Garshev, A. V.; Frantti, J.; Lebedev, O. I.; Churagulov, B. R.; Van Tendeloo, G.; Yoshimura, M. *J. Phys. Chem. B* **2006**, *110*, 4030.
(29) Armstrong, A. R.; Armstrong, G.; Canales, J.; García, R.; Bruce, P. G. *Adv. Mater.* **2005**, *17*, 862.
(30) Grey, I. E.; Li, C.; Madsen, I. C.; Watts, J. A. *J. Solid State Chem.* **1987**, *66*, 7.
(31) Grey, I. E.; Madsen, I. C.; Watts, J. A.; Bursill, L. A. *J. Solid State Chem.* **1985**, *58*, 350. Sugita, M.; Tsuji, M.; Abe, M. *Bull. Chem. Soc. Jpn.* **1990**, *63*, 1978.

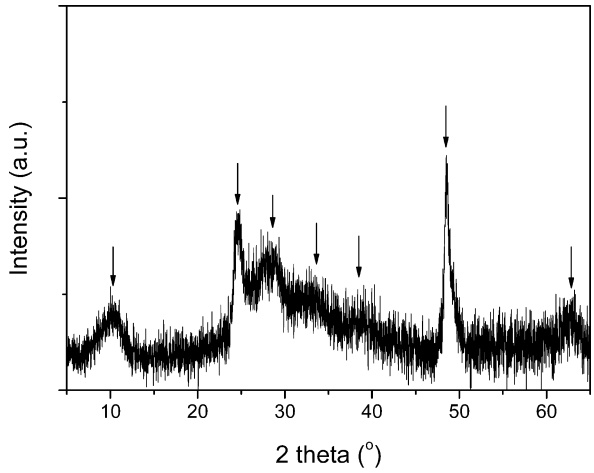

Figure 1. Typical powder XRD pattern of the as-prepared titanate nanotubes. Arrows indicate the observed possible reflections.

cm^{-1}). Raman scattering spectra were collected in a backscattering configuration. The samples were illuminated by using a 632.8 nm He−Ne laser on an Olympus BX 40 confocal microscope with a 50× objective. A cooled charge-coupled device detector was used to collect the scattered light dispersed by a 1800 lines/mm grating. The wavenumber stability and the accuracy of the apparatus were checked by recording the Raman spectrum of silicon. A laser power of 1 mW was used, as it is low enough to prevent damage to the samples but is sufficient to produce good-quality spectra in a reasonable time (30−60 s; two cycles). The Raman scattering spectra with a resolution of about 2 cm^{-1} were collected at room temperature.

Results and Discussion

Figure 1 shows a typical powder XRD pattern of the product after hydrothermally treating anatase TiO_2 powders in 10 M NaOH aqueous solution at 140 °C for 24 h and subsequent acid washing. The XRD pattern is basically the same as those reported previously for titanate nanotubes,[10−18] implying that the identical nanotubular structure is obtained in this work. The broad peak at $2\theta = 10.23°$ corresponding to a d spacing of 0.86 nm is generally attributed to the interlayer diffraction of the as-prepared titanate nanotubes.[10−18] Note that there are only a few broad XRD reflections; any unequivocal indexing of the XRD pattern to any known titanate polymorph is thus impossible. The measured d values are reported in Table 1, in which all possible titanate models proposed in the literature are also tabulated for comparison.

Figure 2 reports the morphology and the microstructure of the as-prepared titanate nanotubes. As demonstrated by the SEM images, the wet chemical method enables mass production of the titanate nanotubes with high purity.[1] TEM observation reveals that the titanate nanotubes have almost uniform inner diameters of about 5 nm and outer diameters of about 11 nm. Lengths of the nanotubes range from several tens to several hundreds of nanometers. An ED pattern taken from an area that contains many nanotubes is shown in the inset of Figure 2c. Diffraction rings are observed since the sample is polycrystalline with many nanotubes oriented randomly. Note that there are only two sharp diffraction rings, corresponding to the two intensive reflections (d = 3.612 and 1.872 Å) in the XRD pattern, see Figure 1 and Table 1; the rest of the ED rings are very obscure. The high-resolution TEM image (Figure 2d) indicates that the nanotubes are usually three to five layers in walls with a typical interlayer distance of about 0.8 nm, in agreement with the XRD data (Figure 1). Note that the layer numbers on either side of the nanotubes are usually not equal, suggesting that the nanotubes were formed by rolling the lamellar intermediates. The presence of a small amount (less than 5%) of sheetlike byproduct (Figure 2d) seems in harmony with this assumption.

Table 1. Comparison of Structural Parameters of the Titanate Nanotubes to Those of the Protonic Titanates (Å)

nanotubes	$H_2Ti_3O_7$[a]		$H_2Ti_4O_9 \cdot H_2O$[b]		$H_2Ti_2O_5 \cdot H_2O$[c]		$H_{0.7}Ti_{1.825}\square_{0.175}O_4 \cdot H_2O$[d,e]	
$d_{measured}$	d	$h\,k\,l$	d	$h\,k\,l$	d	$h\,k\,l$	d	$h\,k\,l$
8.623	7.87	2 0 0	9.05	2 0 0	9.04	2 0 0	9.272	0 2 0
3.612	3.65	1 1 0	3.672	1 1 0	3.696	1 1 0	3.707	1 1 0
3.137	3.05	3 1 0	3.185	3 1 0	3.204	3 1 0	3.226	1 3 0
2.68	2.67	3 1 −2	2.668	2 1 −3	2.684	3 0 1	2.686	0 3 1
2.305	2.37	1 1 −3	2.298	2 1 −4	2.306	5 0 1	2.324	0 5 1
1.872	1.88	0 2 0	1.876	0 2 0	1.893	0 2 0	1.891	2 0 0
1.474					1.478	2 0 2	1.491	0 0 2

[a] JCPDS 47-0561; monoclinic; a = 16.023, b = 3.749, c = 9.191, and β = 101.45°. [b] JCPDS 36-0655; monoclinic; a = 18.77, b = 3.75, c = 11.62, and β = 104.6°. [c] JCPDS 47-0124; orthorhombic; a = 18.03, b = 3.783, and c = 2.998. [d] Calculated from JCPDS 83-0702; orthorhombic; a = 3.783, b = 18.545, and c = 2.982. [e] A similar compound is reported in ref 22, with lattice parameters of a = 3.801, b = 18.880, and c = 3.076.

The nanotubular structure of the as-prepared products was characterized further by nitrogen isothermal adsorption at 77 K. A typical isotherm for nitrogen adsorption on the surfaces of the nanotubes is shown in Figure 3. These isotherms exhibit obvious hysteresis behavior, revealing that the products are mainly mesoporous. According to the BET equation, the surface area of the as-prepared titanate nanotubes is about 200 m^2/g. The pore size distribution was analyzed by using the BJH method. The BJH desorption pore volume is 0.56 cm^3/g with a peak pore position around 3.53 nm. These data are in good agreement with the published values of the titanate nanotubes.[32]

The high surface area and the mesoporous structure of the titanate nanotubes imply a strong tendency to absorb water from the washing solution or from the ambient atmosphere.[12] The amount of adsorbed water was determined by TGA (Figure 4). The titanate nanotubes undergo dehydration in two overlapping steps with different dehydration rates, 40−150 °C (step I) and 150−450 °C (step II), for which the corresponding weight loss is approximately 9% and 4%, respectively. No further weight loss is observed up to 600 °C. Usually, the weight loss of step I corresponds to the evaporation of free water molecules in the nanotubes, which is dependent on the synthetic conditions.[12] The weight loss in step II can be attributed to the dehydroxylation of the nanotubes and the formation of anatase. As shown in Table 2, different protonic titanates will give different weight losses as they transform into anatase (note that we consider only

(32) Bavykin, D. V.; Parmon, V. N.; Lapkin, A. A.; Walsh, F. C. *J. Mater. Chem.* **2004**, *14*, 3370. Tsai, C. C.; Teng, H. *Chem. Mater.* **2004**, *16*, 4352.

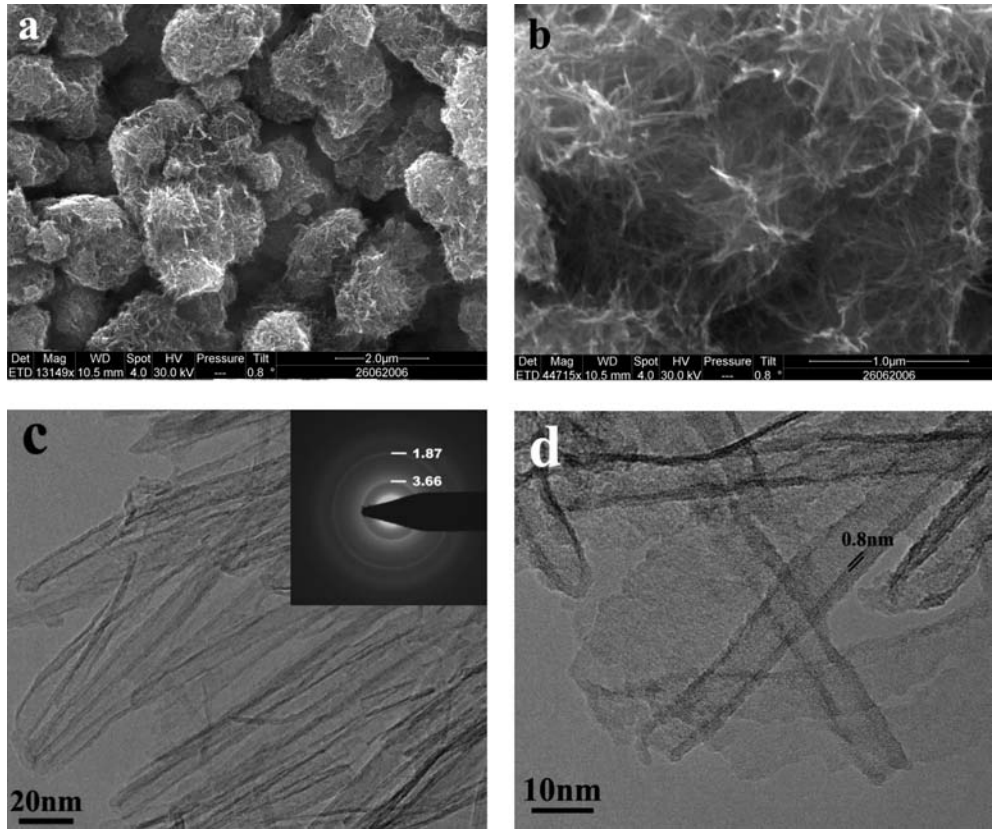

Figure 2. SEM (a and b) and TEM (c and d) images of the as-prepared titanate nanotubes. Inset of c shows an electron diffraction pattern (Å).

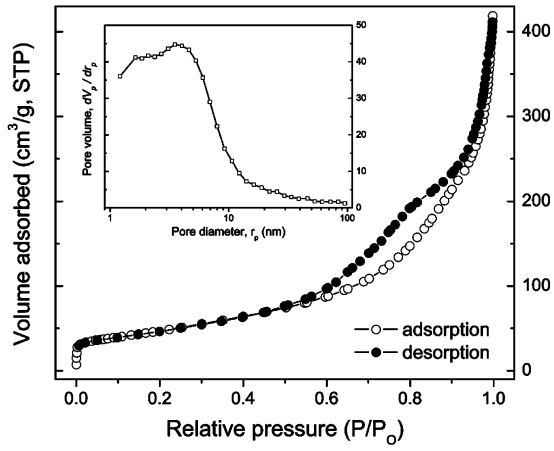

Figure 3. Isotherm of low-temperature nitrogen adsorption and desorption of titanate nanotubes. The inset shows a pore volume distribution (BJH desorption).

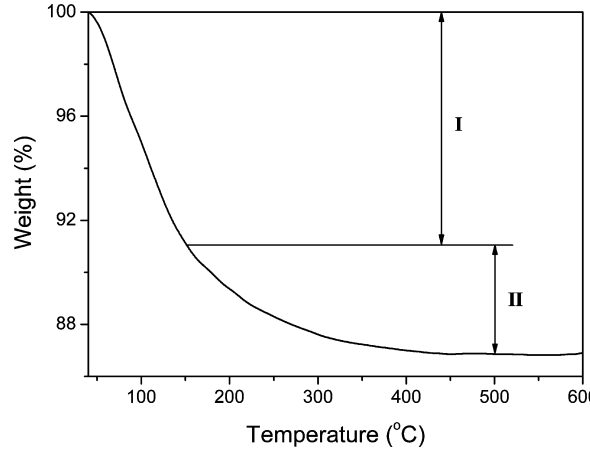

Figure 4. TGA curve of the as-prepared titanate nanotubes measured at a heating rate of 5 °C/min under N_2 flow.

the dehydroxylation reaction, which is independent of the synthetic conditions). These structural data have to be taken into account before a structural model of the titanate nanotubes can be proposed. For example, the protonic titanate $H_2Ti_2O_5 \cdot H_2O$ (or $H_2Ti_2O_4(OH)_2$)[16,17] is supposed to have similar lepidocrocite-type host layers to those in the layered titanate $H_{0.7}Ti_{1.825}\square_{0.175}O_4 \cdot H_2O$.[17,22,31] Considering its exceptional weight loss upon the formation of anatase (Table 2), we suggest that the protonic titanate $H_2Ti_2O_5 \cdot H_2O$ did not represent a better structural basis for the titanate nanotubes in comparison with the lepidocrocite titanate $H_{0.7}Ti_{1.825}\square_{0.175}O_4 \cdot H_2O$.[18]

Table 2. Expected Weight Loss of Dehydrated Titanates upon the Formation of Anatase

compounds	expected weight loss (wt %)
$H_2Ti_3O_7$	6.98
$H_2Ti_4O_9$	5.33
$H_2Ti_2O_5$	10.12
$H_{0.7}Ti_{1.825}\square_{0.175}O_4$	4.14

The as-prepared titanate nanotubes were characterized also by means of FT-IR and Raman scattering spectroscopy to understand their local structural properties. As shown in Figure 5a, the FT-IR spectrum of the titanate nanotubes is featureless and shows mainly absorption bands related to water molecules. For example, the broad band at about 3300 cm^{-1} and a prominent absorption at 1626 cm^{-1} are due to

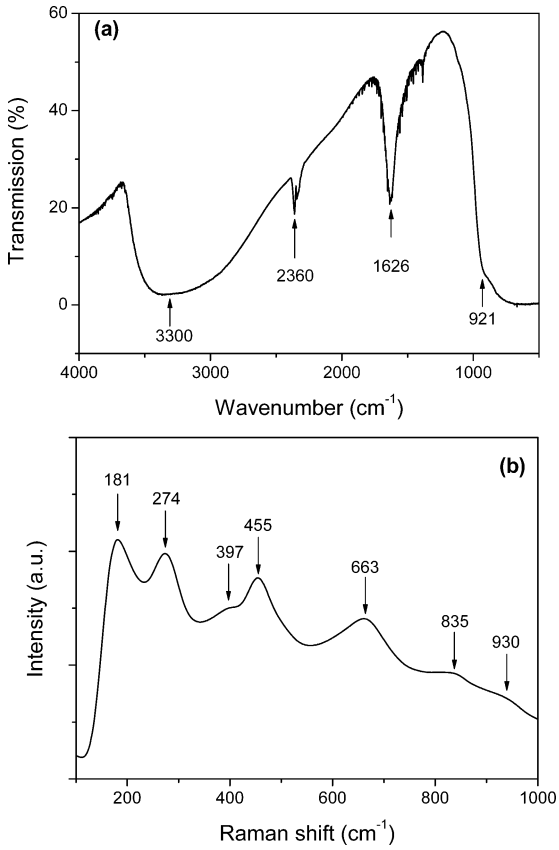

Figure 5. Vibrational spectroscopic data of the titanate nanotubes. (a) IR and (b) Raman scattering.

stretching and bending vibrations of H_2O (or H_3O^+), respectively.[33] The presence of free water molecules is consistent with the TGA data (Figure 4). The absorptions at 2360 and 921 cm^{-1} are due to CO_2 from the ambient atmosphere and Ti−O lattice vibrations, respectively. In contrast, the Raman scattering spectrum, Figure 5b, of the as-prepared titanate nanotubes features several well-defined Raman bands at 181, 274, 397, 455, 663, 835, and 930 cm^{-1}. Note that the Raman scattering data obtained in this work are consistent with the published values.[1,8,12,18,23−25]

The interpretation of the Raman scattering spectrum of the titanate nanotubes (Figure 5b) can be done by either determining the symmetry properties of the Raman bands or assigning the observed frequencies to vibrations of defined atoms or groups of atoms: they do not exclude each other. Owing to the large difference among the atomic masses of Ti, O, and H, it is reasonable to assume that the observed phonons are almost pure modes; that is, they mainly involve displacements of a single atomic species. Furthermore, it is generally correct that phonons involving displacements of light ions have large wavenumbers. Therefore, it is reasonable that the Raman bands in Figure 5b involve mainly the Ti−O vibrations and do not include a significant contribution from the water species.[26] So far, the interpretation of the Raman scattering data of the titanate nanotubes has been performed by considering mainly the Ti−O lattice vibrations. For example, the Raman band at about 930 cm^{-1} has been assigned to a four-coordinate Ti−O vibration by Kasuga et al.[1] or to a short symmetric Ti−O stretching mode by Menzel et al.[25] The Raman bands at 181, 397, and 663 cm^{-1} have generally been attributed to Ti−O vibrations of anatase.[1,24,25] Although the Raman band at 274 cm^{-1} has been recognized as an intrinsic mode related to the new titanate phases,[24] its origin has not been explored so far.

An analysis of the Raman scattering data of a material in terms of symmetry properties is generally necessary for its structural identification. To achieve this for the titanate nanotubes, it is helpful to consider first the Raman scattering data of crystalline TiO_2, that is, anatase and rutile. Structurally, the anatase-phase TiO_2 is tetragonal, space group $I41/amd$.[34] The lattice contains two formula groups per unit cell and 10 optical phonons of symmetry $A_{1g} + A_{2u} + 2B_{1g} + B_{2u} + 3E_g + 2E_u$, of which A_{1g}, $2B_{1g}$, and $3E_g$ are Raman-active; A_{2u} and $2E_u$ are IR-active; and B_{2u} is inactive in both Raman and IR spectra.[35] As shown in Figure 6a, the Raman scattering spectrum of the anatase-phase TiO_2 has five typical contributions at 146(E_g), 199(E_g), 398(B_{1g}), 517(B_{1g}/A_{1g}), and 641(E_g) cm^{-1}, in good agreement with the theoretical analysis and the published data.[36] On the other hand, rutile-phase TiO_2 is tetragonal, space group space group $P4_2/mnm$, with two molecules per unit cell.[34] The lattice contains 10 optical phonons of symmetry $A_{1g} + A_{2g} + A_{2u} + B_{1g} + B_{2g} + E_g + 2B_{1u} + 3E_u$, of which A_{1g}, B_{1g}, B_{2g}, and E_g are Raman-active; A_{2u} and $3E_u$ are IR-active; and A_{2g} and $2B_{2u}$ are inactive in both Raman and IR spectra.[35,37] The Raman scattering spectrum of the rutile-phase TiO_2 is shown in Figure 6b, in which the three first-order phonons are recorded at 828(B_{2g}), 612(E_g), and 449(A_{1g}) cm^{-1}; the Raman band at 237 cm^{-1} belongs to second-order Raman scattering.[38] It is important to point out that both anatase and rutile are composed of similar TiO_6 octahedra with similar Ti−O band lengths,[34] of which the different polymerization types of the TiO_6 octahedra (Figure 6c and d) are obviously responsible for their different vibrational properties (Figure 6a and 6b). Comparing the Raman scattering data of the titanate nanotubes (Figure 5b) with those of the crystalline TiO_2 (Figure 6a and b), one can conclude that the titanate nanotubes are actually not crystalline TiO_2 (anatase or rutile) as proposed previously.[1,8,9] That is to say, the TiO_6 octahedra in the nanotubular framework (i.e., titanate nanotubes) must possess a very different polymerization nature from those in anatase or rutile.

Then, we consider the Raman scattering properties of different bulky layered titanates that are proposed to be the structural basis of the titanate nanotubes. Considering the crystalline structure of the layered titanates first, one may

(33) Fadini, A.; Schnepel, F. M. *Vibrational Spectroscopy: Methods and Applications*; Ellis Horwood Limited: England, 1989.

(34) Burdett, J. K.; Hughbanks, T.; Miller, G. J.; Richardson, J. W., Jr.; Smith, J. V. *J. Am. Chem. Soc.* **1987**, *109*, 3639.

(35) Fateley, W. G.; Dollish, F. R.; McDevitt, N. T.; Bentley, F. F. Infrared and Raman Selection Rules for Molecular and Lattice Vibrations: *The Correlation Method*; Wiley-Interscience: New York, 1972.

(36) Su, W.; Zhang, J.; Feng, Z.; Chen, T.; Ying, P.; Li, C. *J. Phys. Chem. C* **2008**, *112*, 7710. Ohsaka, T.; Izumi, F.; Fujiki, Y. *J. Raman Spectrosc.* **1978**, *7*, 321.

(37) Matossi, F. *J. Chem. Phys.* **1951**, *19*, 1543. Traylor, J. G.; Smith, H. G.; Nicklow, R. M.; Wilkinson, M. K. *Phys. Rev. B: Condens. Matter Mater. Phys.* **1971**, *3*, 3457.

(38) Swamy, V.; Muddle, B. C.; Dai, Q. *Appl. Phys. Lett.* **2006**, *89*, 163118.

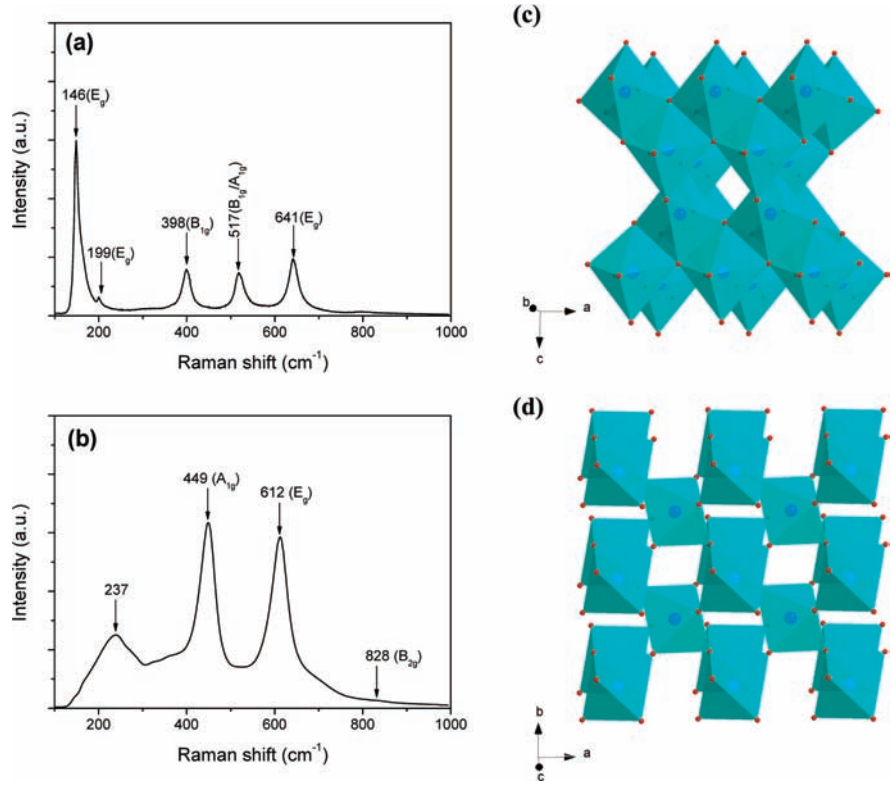

Figure 6. (Color online) Raman scattering data of (a) anatase- and (b) rutile-phase TiO_2. Polyhedral representation of anatase (c) and rutile (d) is shown for comparison.

notice that the monoclinic titanates ($H_2Ti_3O_7$ or $H_2Ti_4O_9$) and the orthorhombic titanates ($H_2Ti_2O_5 \cdot H_2O$ or $H_{0.7}Ti_{1.825}\square_{0.175}O_4 \cdot H_2O$) are very different.[18,20,22] For example, the crystal structure of the lepidocrocite titanate $H_{0.7}Ti_{1.825}\square_{0.175}O_4 \cdot H_2O$ is orthorhombic, space group *Immm*, with two $H_{0.7}Ti_{1.825}\square_{0.175}O_4 \cdot H_2O$ formula units per primitive unit cell. Factor group analysis reveals nine Raman lines $3A_g + 3B_{1g} + 3B_{3g}$ corresponding to Ti−O lattice vibrations within the 2D lepidocrocite-type TiO_6 octahedral host layers.[26] These intrinsic Raman modes are reported in Figure 7a. In contrast, the monoclinic $H_2Ti_3O_7$ belongs to space group $P2_1/m$, with two $H_2Ti_3O_7$ formula units per primitive unit cell.[39] All atoms lie in a general position (Wyckoff site 2*e*) with only site symmetry C_s allowed; 69 normal optical phonons $24A_g + 12B_g + 11A_u + 22B_u$ can be readily obtained via factor group analysis. Of these, all gerade modes are Raman-active and all ungerade modes are IR-active. As shown in Figure 7b, at least 14 Raman bands are observed for the monoclinic $H_2Ti_3O_7$, in agreement with the low symmetry of this monoclinic titanate. These difference vibrational properties can also be understood by the different polymerization natures of TiO_6 octahedra in these different compounds. For example, the host layers of lepidocrocite titanate $H_{0.7}Ti_{1.825}\square_{0.175}O_4 \cdot H_2O$ are "flat", in which the TiO_6 octahedra are combined with each other via edge-sharing,[27,40] as shown in Figure 7c. On the other hand, the crystal structure of $H_2Ti_3O_7$ is composed of corrugated ribbons of edge-sharing TiO_6 octahedra; the ribbons are three-octahedra-wide. These octahedra join at the corners to form a "stepped" layered structure, as shown in Figure 7d.[20,22,39] Comparing the Raman scattering data of the titanate nanotubes (Figure 5b) with those of the bulky layered titanates (Figure 7a and b), one may find that the protonic titanate $H_{0.7}Ti_{1.825}\square_{0.175}O_4 \cdot H_2O$ represents an ideal structural basis for the titanate nanotubes. This is also supported by other structural information like TGA (Figure 4 and Table 2) as well as the detailed diffraction studies (XRD, TEM, ED, etc.) reported previously by Ma et al.[18]

It should be pointed out that the formation of the titanate nanotubes may involve the scrolling of the 2D titanate nanosheets (i.e., the lamellar intermediates); the corresponding Ti−O bond lengths and bond angles are supposed to be changed as the layers are bent. Although the details of these local structural evolutions are still not clear, it is generally correct that Raman scattering properties of the titanate nanotubes would be different somewhat from those of the 2D titanate nanosheets as well as those of the bulky layered titanates. These differences have to be taken into account as the crystal structures of the titanate nanotubes are discussed via Raman scattering spectroscopy or other methods such as XRD, ED, and PDF simulations.

Since the 1D scroll-like titanate nanotubes can be unscrolled into corresponding 2D titanate nanosheets,[27] it is possible to assemble a 3D bulky titanate by employing the unscrolled nanosheets as building blocks, as shown in Scheme 1. This unscrolling−restacking reaction can be understood as follows. The unscrolled 2D titanate nanosheets are covered with positive-charged amine cations with large diameters.[27] The ionic strength of the colloidal nanosheet

(39) Andersson, S.; Wadsley, A. D. *Acta Crystallogr.* **1961**, *14*, 1245.
(40) Sasaki, T.; Watanabe, M.; Michiue, Y.; Komatsu, Y.; Izumi, F.; Takenouchi, S. *Chem. Mater.* **1995**, *7*, 1001.

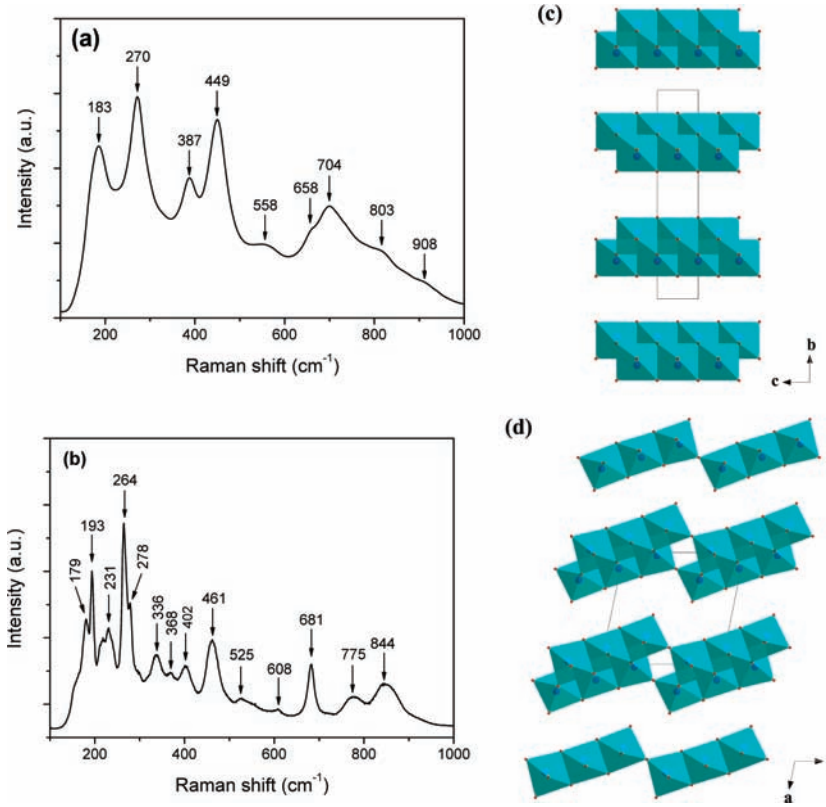

Figure 7. (Color online) Raman scattering data of (a) orthorhombic $H_{0.7}Ti_{1.825}\square_{0.175}O_4 \cdot H_2O$ and (b) monoclinic $H_2Ti_3O_7$. Polyhedral representation of (c) $H_{0.7}Ti_{1.825}\square_{0.175}O_4 \cdot H_2O$ and (d) $H_2Ti_3O_7$ is shown for comparison. The titanium site vacancies in part c are not shown for simplification. Interlayer water molecules (H_2O/H_3O^+) are not shown. Solid lines encircle the unit cell.

Scheme 1. Proposed Unscrolling-Restacking Process for Titanate Nanotubes

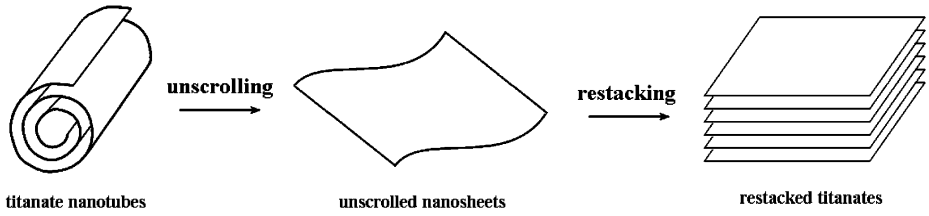

solution will be changed as foreign cations are introduced.[41] Subsequently, the bulky organic amine ions (TMA in this study) will be replaced by the smaller inorganic cations (H^+, K^+, or Na^+ ions), resulting in dramatic environmental changes of the 2D titanate nanosheets. The titanate nanosheets will be either restacked into layered materials or scrolled into nanotubes,[41,42] depending on the lateral sizes of the nanosheets themselves as well as the experimental conditions applied. In this work, only platelike layered materials are obtained (see the Supporting Information), suggesting that the formation of the titanate nanotubes might not follow a simple rolling process as that proposed previously.[9,42] We wish to make it clear that the polymerization nature of the TiO_6 octahedra in the nanotubular framework (i.e., titanate nanotubes) will be the same as that in this restacked titanate. In this regard, the Raman scattering properties and consequent crystal structures of the titanate nanotubes can be understood by considering those of the restacked titanates.

Figure 8 shows the general morphology of the restacked titanate, in which platelike crystallites with typical lateral sizes of several micrometers can be seen clearly. The thickness of the restacked materials ranges from tens of nanometers up to 2 μm (inset of Figure 8b). These structural data suggest that the restacking of the unscrolled titanate nanosheets was rather random along both lateral and thickness directions.

The restacked titanate is poorly crystallized, as evidenced by the XRD data shown in Figure 9a; structural identification via the diffraction methods is therefore difficult. On the other hand, several Raman bands are observed in the restacked materials, as shown in Figure 9b. Note that the restacked titanates inherit the same polymerization nature of the TiO_6 octahedra as that in the nanotubular framework (i.e., titanate nanotubes). Consequently, the Raman scattering data of the restacked titanate are supposed to be similar to those of the protonic titanate $H_{0.7}Ti_{1.825}\square_{0.175}O_4 \cdot H_2O$ (Figure 7a).[26] This is actually observed in the present study; the corresponding Raman scattering data are reported in Table 3 for comparison.

(41) Saupe, G. B.; Waraksa, C. C.; Kim, H. N.; Han, Y. J.; Kaschak, D. M.; Skinner, D. M.; Mallouk, T. E. *Chem. Mater.* **2000**, *12*, 1556.
(42) Ma, R.; Bando, Y.; Sasaki, T. *J. Phys. Chem. B* **2004**, *108*, 2115.

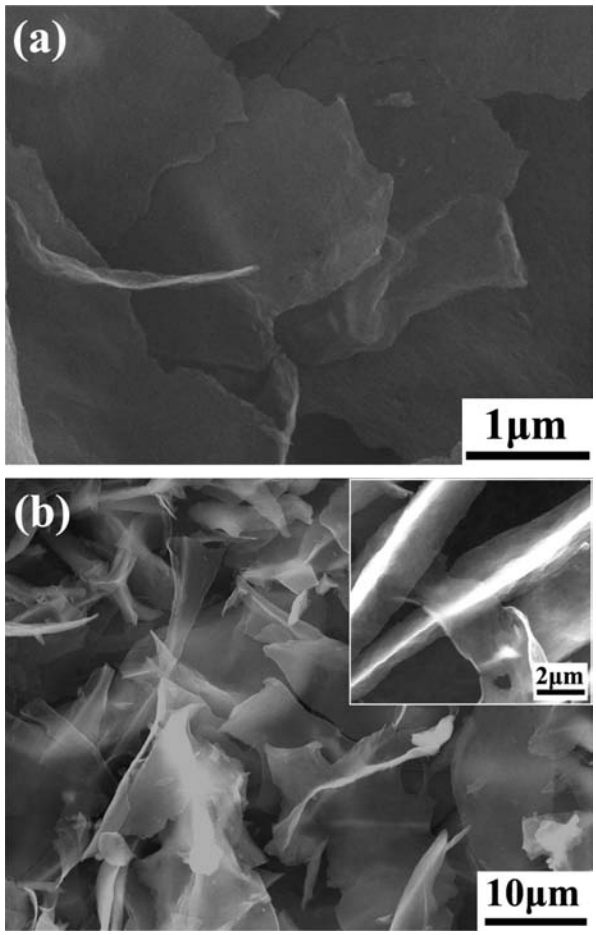

Figure 8. SEM images of the restacked titanate.

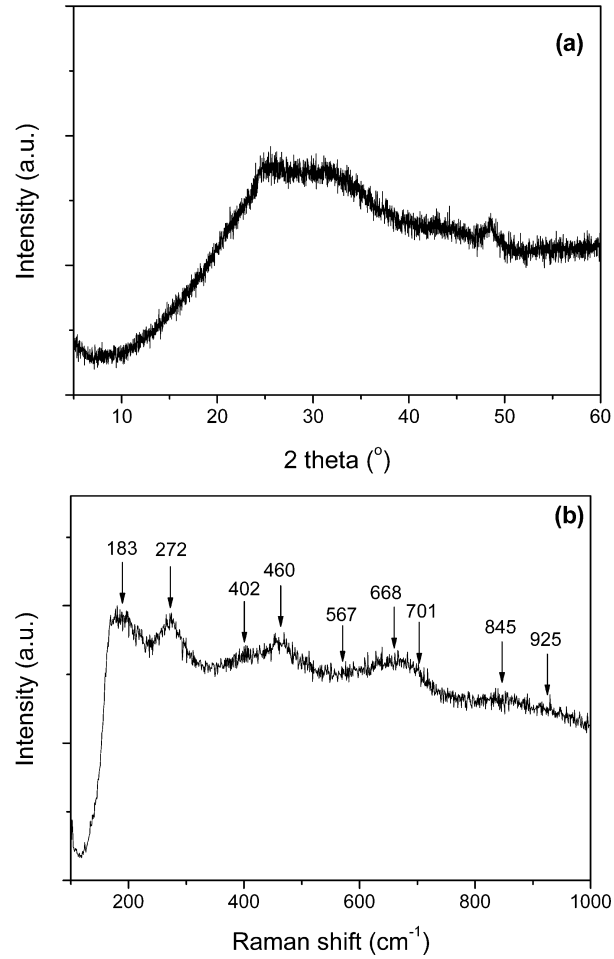

Figure 9. (a) XRD pattern and (b) Raman scattering data of the restacked titanate.

The similarity of the Raman scattering spectrum of the titanate nanotubes (Figure 5b) to that of the lepidocrocite-type titanate (Figure 7a) and the restacked titanate (Figure 9b) indicates that the protonic titanate $H_{0.7}Ti_{1.825}\square_{0.175}O_4 \cdot H_2O$ represents an ideal structural basis for the titanate nanotubes. Raman scattering properties of the protonic titanate $H_{0.7}Ti_{1.825}\square_{0.175}O_4 \cdot H_2O$ have been discussed previously,[26] of which three A_g symmetric modes corresponding to pure framework Ti−O−Ti vibrations are recorded at about 270, 449, and 704 cm^{-1}. In this work, these symmetric A_g modes are observed at about 272, 460, and 701 cm^{-1} in the restacked titanate. Consequently, the intensive Raman bands at about 274, 454, and 663 cm^{-1} in the titanate nanotubes (Figure 5b) can be assigned to the A_g modes, revealing the presence of the 2D lepidocrocite-type TiO_6 octahedral layers. The high wavenumber A_g mode at 663 cm^{-1} of the titanate nanotubes shows a remarkable band shift in comparison with that of the bulky titanates, 704 cm^{-1}. This can be attributed to the bending of the TiO_6 octahedral layers during the rolling process. It is interesting as well as important to point out that the scroll-like titanate nanotubes do not possess the radial breathing vibrations that are normally present in the cylinder-like nanotubes with a closed shell structure such as carbon nanotubes.[43] Clearly, different physicochemical properties can be expected in these two different nanotubular systems.[27]

A question still remains. As shown in Figure 1 and Table 1, the first XRD peak at $2\theta = 10.23°$ ($d = 0.86$ nm) and the most intensive XRD peak at $2\theta = 48.59°$ ($d = 0.187$ nm) of the titanate nanotubes are usually assigned to the (020) and (200) planes, respectively, of the protonic titanate $H_{0.7}Ti_{1.825}\square_{0.175}O_4 \cdot H_2O$.[18] This indicates that, to form nanotubes, the 2D lepidocrocite-type TiO_6 octahedral layers would bend along the [001] direction (i.e., *c* axis) of the orthorhombic structure with the tube axis along the [100] direction (i.e., *a* axis). However, it is an energy-intensive process: the rolling of the layers along the *a* axis is supposed to be very convenient since there are ridges and troughs in the 2D

Table 3. Raman Scattering Data of the Titanate Nanotubes, the Protonic Titanate $H_{0.7}Ti_{1.825}\square_{0.175}O_4 \cdot H_2O$, and the Restacked Titanate (cm^{-1})

titanate nanotubes	$H_{0.7}Ti_{1.825}\square_{0.175}O_4 \cdot H_2O$	restacked titanate
180	183	183
274	270	272
396	387	402
454	449	460
	558	567
663	658	668
	704	701
835	803	845
930	908	925

(43) Dresselhaus, M. S.; Dresselhasu, G.; Saito, R.; Jorio, A. *Phys. Rep.* **2005**, *409*, 47. Dersselhaus, M. S.; Dresselhasu, G.; Hofman, M. *Philos. Trans. R. Soc. London, Ser. A* **2008**, *366*, 231. Kudin, K. N.; Ozbas, B.; Schniepp, H. C.; Prud'homme, R. K.; Aksay, I. A.; Car, R. *Nano Lett.* **2008**, *8*, 36.

lepidocrocite-type TiO_6 octahedral layers along the *c* axis (Figure 7c). Similar phenomena can also be found in other orthorhombic titanates such as $H_2Ti_2O_4(OH)_2$)[16] and $H_2Ti_2O_5 \cdot H_2O$.[17] This may be explained by the fact that the formation of the titanate nanotubes proceeds via not a simple rolling process[9,22,42] but a complex self-assembly process in hot, concentrated alkali solutions.[44] The formation of the vacancy seems common when isolated TiO_6 octahedra are rearranged into lepidocrocite-type TiO_6 octahedral layers. Moreover, the presence of vacancies is necessary to release the stress as the octahedral layers are subsequently scrolled into nanotubes. Further studies are still necessary for the details.

Conclusions

In summary, from a viewpoint of vibrational spectroscopy, we discuss the crystal structures of the titanate nanotubes prepared from a NaOH treatment of TiO_2 with subsequent washing. The titanate nanotubes show seven Raman bands at 180, 274, 396, 454, 663, 835, and 930 cm^{-1}, which can be assigned to Ti−O lattice vibrations within lepidocrocite-type TiO_6 octahedral host layers. We demonstrate that the crystal structure of the titanate nanotubes can be better described by the protonic titanate $H_{0.7}Ti_{1.825}\square_{0.175}O_4 \cdot H_2O$. Since different titanate structures can be produced via the alkaline treatment of crystalline TiO_2 under different conditions,[14,18,26,27] the application of Raman scattering spectroscopy seems interesting and necessary to collect sufficient evidence for a reliable description on the microstructure of the final products.

Acknowledgment. We thank Dr. Frank Krumeich and Prof. Reinhard Nesper (Laboratory of Inorganic Chemistry, ETH Zurich) for their help on TEM analysis. The authors would like to acknowledge financial assistance from the Research Council of Norway through the NANOMAT program (163565-431).

Supporting Information Available: SEM, XRD, and Raman scattering data of some layered titanates and restacked titanates (PDF file). This material is available free of charge via the Internet at http://pubs.acs.org.

IC801508K

(44) Kukovecz, Á; Hodos, M.; Horváth, E.; Radnóczi, G.; Kónya, Z.; Kiricsi, I. *J. Phys. Chem. B* **2005**, *109*, 17781.